condition is thought to be brought about by the unusual results of lag mode eigenvalues at layer angles of -10 to -30 deg.

Concluding Remarks

In this work, the effects of transverse shear on the aeroelastic analysis of a composite rotor having antisymmetric configuration have been investigated by using the finite element method. The results shown in this article reveal that, for this type of configuration, the incorporation of transverse shear influenced the system on both the frequency and damping in a dramatic manner: instabilities occurred at several ply orientation angles. So it is vital from the analysis that the transverse shear flexibility (considering the distribution of shear) should be kept for the analysis of composite rotor to get more enhanced results.

References

[1] Whitney, J. M., "Shear Correction Factors for Orthotropic Laminates Under Static Load," *Journal of Applied Mechanics*, Vol. 40, March 1973, pp. 302–304.

[2] Rehfield, L. W., Atilgan, A. R., and Hodges, D. H., "Nonclassical Behavior of Thin-Walled Composite Beams with Closed Cross Sections," *Journal of the American Helicopter Society*, Vol. 35, No. 2, 1990, pp. 42–50.

[3] Hong, C. H., and Chopra, I., "Aeroelastic Stability Analysis of a Composite Rotor Blade," *Journal of the American Helicopter Society*, Vol. 30, No. 2, 1985, pp. 57–67.

[4] Hodges, D. H., and Dowell, E. H., "Nonlinear Equations of Motion for the Elastic Bending and Torsion of Twisted Nonuniform Blades," NASA TN D-7818, Dec. 1974.

[5] Smith, E. C., and Chopra, I., "Aeroelastic Response, Loads and Stability of a Composite Rotor in Forward Flight," *AIAA Journal*, Vol. 31, No. 7, 1993, pp. 1265–1273.

[6] Jung, S. N., and Kim, S. J., "Aeroelastic Response of Composite Rotor Blades Considering Transverse Shear and Structural Damping," *AIAA Journal*, Vol. 32, No. 4, 1994, pp. 820–827.

Effects of Boundary Conditions on Postbuckling of Compressed, Symmetrically Laminated Thick Plates

Erasmo Carrera* and Michele Villani†

Politecnico di Torino, 10129 Torino, Italy

I. Introduction

CURRENT metal aircraft design practices allow the skin of some structural components (e.g., fuselage, wing, and stabilizer panels) to buckle at load levels below the design ultimate loading condition. In fact, these structural elements are designed to have a postbuckling strength; evidently a better understanding of the postbuckling behavior of composite panels constitutes an essential requirement toward a rational employment of their strength. Both their ultimate loading conditions and failure characteristics must be well understood.

Boundary conditions play a fundamental role in nonlinear analysis of laminated panels as well as of metallic, isotropic ones. In fact, buckling and postbuckling behavior is very much affected by them. Many examples and exhaustive overviews can be found in the report by Leissa[1] for buckling and in the Chia's book[2] for postbuckling. These two works discuss results related to the classical Kirchhoff's plate approximations classical lamination theory (CLT). The interest in these subjects is also displayed by the many experimental

research activities that were carried out in many laboratories all over the world; as example and for literature we cite the work by Starnes et al.[3] and more recently that by Chai et al.[4]

Usually these experiments are very expensive and the cost of a parametric study becomes prohibitive. Laminated structures exhibit higher transverse deformability in respect to that of metallic ones. In fact, thickness and orthotropic ratio increasing the shear deformation cannot be neglected; further it assumes much more importance in the large deflections field. Some aspects related to first shear deformation theory (FSDT) and nonlinear analysis of composite plates were overviewed by Chia,[5] whereas effects related to higher order shear deformation theory (HSDT) have been recently considered and reviewed by Librescu and Stein[6] and Librescu and Chang.[7] Because of both the limitations of the analytical methods as those in Refs. 1–7 and the high cost of experiments, only a limited amount of data has been published to describe the postbuckling behavior of composite flat panels. These data are even less when shear deformable plates are considered and different boundary conditions are treated. The progress made by approximated methods of the computational mechanics and particularly by the finite element method (FEM) as tools to trace the nonlinear response of many different problems has been recently pointed out by Crisfield.[8] Furthermore the difficulties and/or limitations of the analytical methods to consider different geometrical and mechanical boundary conditions are easily subjugated. On the other hand FEM formulations (especially when concern plates and shells) are very often affected by numerical deficiencies as locking. Fortunately these weaknesses can be overcome by implementation of some strategies as those discussed by Dvorkin and Bathe.[9]

The present work is a sequel to the work of Carrera[10–15] directed to investigate composite plates by FEM. It uses a shear deformable plate finite element of Reissner–Mindlin type. Nonlinearities of von Kármán type are included (large rotations, large strains, and material nonlinearities are not considered). To obtain low bandwidth of FEM stiffnesses matrices, the simple four node plate element Q4 is employed. The numerical efficiency of this element has been reached by application of assumed shear strain field concept discussed by Dvorkin and Bathe[9] among the others. The multilayered formulation of this element was proposed by Carrera in Refs. 13 and 15 and implemented in the FEM code MATCO, which is available at Dipartimento di Ingegneria Aeronautica e Spaziale. Elastic flat plates subjected to static conservative loads are considered. Symmetrically anisotropic laminated plates loaded by in-plane axial compression are analyzed. As novelty in respect to the previous works, herein the attention is focused to the effects of boundary conditions. In particular the effects related to stiffeners are studied and the cases of constant distribution of the displacements at the plate loaded edges are compared with results related to a constant distribution of the load at the same edges.

II. Outlines of the Used Finite Element Model

Consider an elastic body subjected to static loads and under prescribed boundary conditions. If the body is assumed to execute an arbitrary set of infinitesimal virtual displacements, from the actual configuration, the principle of virtual displacements states

$$\delta \Psi = \delta W \tag{1}$$

where $\delta \Psi$ is the virtual variation of the strain energy and δW is the virtual variation of the external work. Upon application of FEM approximations, the variational equation (1) then reduces to a nonlinear set of algebraic equations that we write in the two following equivalent forms[12]:

$$\{\varphi(\{q\}, \{p\})\} = 0; \qquad [K_S(\{q\})]\{q\} = \{p\} \tag{2}$$

where $\{q\}$ is the n-dimensional vector of the nodal displacements and/or rotations, $\{\varphi\}$ is the n-dimensional vector of the resultant nodal forces (inner plus external forces), $\{p\}$ is the n-dimensional vector of the nodal forces equivalent to the external loads (which is assumed deformation independent), and $[K_S]$ is the secant stiffness matrix. (Brace and square brackets denote vectors and matrices, respectively. We refer to the displacements formulation of the FEM.) Equation (2) constitutes the point of departure for finite element

calculation of geometrically nonlinear systems. In addition it is assumed that the structure is subjected to a proportional loading, i.e., $\{p\} = \lambda\{f\}$, where $\{f\}$ denotes a fixed reference load vector and λ is a load-scaling factor, load parameter. A standard solution scheme for Eq. (2) is obtained through the following straightforward application of the Newton's method between the initial state i and the unknown state $i + 1$ (in the neighborhood of i):

$$\{\varphi_{res}\} = [\{\varphi\}_{,\{q\}}]\{\Delta q\} + [\{\varphi\}_{,\{p\}}]\{\Delta p\} \tag{3}$$

in which the load level is treated as a variable; the notation $,_{..}$ denotes partial derivative. Within the limits of our assumptions we have $\{\Delta p\} = \Delta\lambda\{f\}$, $\{\varphi_{,\{q\}}\} = [K_T(\{q^i\})]$, and $\{\varphi_{,\{p\}}\} = -[I]$, where $[K_T]$ is the tangent stiffness matrix, $[I]$ is the unit matrix, $\{\Delta q\} = \{q^{i+1}\} - \{q^i\}$ is the incremental nodal displacement vector, $\Delta\lambda = \lambda^{i+1} - \lambda^i$ is the incremental load factor, and $\{\varphi_{res}\} = [K_S\{q^i\}]\{q^i\} - \lambda^i\{f\}$ is the residual nodal vector of the nodal forces (unbalanced nodal forces vector). Upon substitution of the previous notations, the incremental Eq. (3) becomes

$$[K_t]\{\Delta q\} = \{\varphi_{res}\} + \Delta\lambda\{f\} \tag{4}$$

Since the load level λ is treated as a variable, an extra governing equation is required and this is given by a constraint relationship of the form $c(\{\Delta q\}, \Delta\lambda)$. This constraint equation is method dependent: several forms of the constraint equation have been proposed by the FEM literature. In the numerical investigation we refer to the modified form of the arc-length-type constraint proposed by Carrera.[12] In numerical investigations we refer to the plate element detailed described in Refs. 10 and 13 to which the interested readers are addressed for more details and explicit expression of the introduced matrices. And its concise description follows.

To take into account the effects of the transverse shear deformation, the displacements field is assumed to be of the following Reissner–Mindlin form:

$$u(x, y, z) = u^0(x, y) + z\phi_x(x, y)$$
$$v(x, y, z) = v^0(x, y) + z\phi_y(x, y); \quad w(x, y, z) = w^0(x, y) \tag{5}$$

in which x, y, and z denote the coordinates of a triorthogonal Cartesian reference system (see subsequent Fig. 9); u, v, and w denote the displacements of a generic point along the directions x, y, and z, respectively; u^0, v^0, and w^0 are the displacement components of a point on the reference surface Ω of the plate; ϕ_x and ϕ_y denote the rotations of the normal to the reference surface in the planes x-z and y-z, respectively, in which the rotations due both to bending deflections $(w_{,x}, w_{,y})$ and to shear deformations are included. The displacements field of Eq. (5) permits us to refer to isoparametric formulation. According to this formulation the unknown functions in the domain Ω of the element can be written as the coordinates, in the following form:

$$(u^0, v^0, w^0, \phi_x, \phi_y) = \{N\}^T\{q\} \tag{6}$$

where $\{N\}$ denotes the vector of N_n components (N_n is the number of the nodes whereas the superscript T denotes transposition) which are the shape functions.

We consider a multilayered plate of constant thickness h, consisting of a finite number N_l of thin layers of orthotropic material and uniform thickness perfectly bonded together. The principal axes of elasticity of any individual layer are assumed to be parallel with the laminate axes. The material properties and the thickness of each layer may be entirely different. As usual by neglecting the normal stresses σ_{zz} the constitutive relations for any individual k layer in matrix form hold: $\{\sigma\} = [Q]\{\epsilon\}$. The following nonlinear strain-displacement relations of von Kármán type have been used:

$$\epsilon_{xx} = u_{,x} + \tfrac{1}{2}w_{,x}^2; \quad \epsilon_{yy} = v_{,y} + \tfrac{1}{2}w_{,y}^2$$

$$\epsilon_{xy} = u_{,y} + v_{,x} + w_{,x}w_{,y}; \quad \epsilon_{xz} = u_{,z} + w_{,x} \tag{7}$$

$$\epsilon_{xz} = v_{,z} + w_{,y}$$

Because its low bandwidth, we have restricted the descriptions to a particular case of the $Q4$ finite element. Large literature has shown that numerical tricks such as reduction or selective integration of the stiffness matrix are not sufficient to improve the performances of $Q4$ element. Patch tests have revealed that in large displacements analyses, although reduced integration often causes zero determinant of these matrices, the selective case could lead to solutions oscillating around the equilibrium path. To establish numerical efficiency, the assumed shear strain concept was applied in Ref. 13 to the multilayered plate formulation presented earlier. Based on a mixed interpolation of the tensorial components the method differently treats the shear contribution to the stiffness matrix in respect to those coming from bending and in-plane deformations. The shear stiffness is not computed at the nodes but in correspondence to four sample points M, N, P, and Q (see the sketch inside Fig. 1) according to the following interpolations of the shear strains field:

$$\epsilon_{xz} = \tfrac{1}{2}(1 + \eta)\epsilon_{xz}^P + \tfrac{1}{2}(1 - \eta)\epsilon_{xz}^M$$
$$\epsilon_{yz} = \tfrac{1}{2}(1 + \xi)\epsilon_{yz}^Q + \tfrac{1}{2}(1 - \xi)\epsilon_{yz}^N \tag{8}$$

in which ξ and η denote the natural coordinate on Ω. The theoretical fundamentals of such approximation in relation to mixed concepts are discussed in many published papers; see Dvorkin and Bathe,[9] for example.

III. Results and Discussion

Simply supported (S), clamped (C), and free edges (F) are considered as in the following description: SFSF: $x = 0, a \rightsquigarrow$ free edge; $y = 0, b \rightsquigarrow w = 0$; SSSS: $x = 0, a \rightsquigarrow w = 0$; $y = 0, b \rightsquigarrow w = 0$; CSCS: $x = 0, a \rightsquigarrow w = 0$; $y = 0, b \rightsquigarrow w = \phi_{yz} = 0$; CCCC: $x = 0, a \rightsquigarrow w = \phi_{xz} = 0$; $y = 0, b \rightsquigarrow w = \phi_{yz} = 0$. Analyses have been performed for a cross-ply symmetrically laminate [LAM1: $(0/90)_{symm}$]. By the use of the standard symbols along the orthotropic directions l and t the mechanical properties are $E_l = 40, E_t = 1, G_{lt} = 0.5, G_{tt} = 0.2$, and $\nu = 0.25$. We refer to consistent unit in all of the investigations. Imperfections are simulated by application of transverse disturb loads as a constant distribution of pressure p_{dis}^{z*}. The superscript $*$ denotes components of the reference load vector $\{f\}$ so that, according to Eq. (3), the effective loads are $N_{yy} = \lambda N_{yy}^*$ and $p_{dis}^z = \lambda p_{dis}^{z*}$; N_{yy} denotes the in-plane applied loading, i.e., compression along the y direction. This value corresponds to the resultant force that is uniformly distributed at nodes along the loaded edges of the plate. The value $N_{yy}^* = -30$ is considered in all of the analyses; a, b, and h are the geometric plate dimensions along the x, y, and z directions, respectively. Furthermore, always square plate are analyzed and to highlight the effects of shear deformations all of the results refer to thick plates: $a = b = 140$ and $h = 10$. Additional data of the treated problems are quoted in the captions of the figures. Results related to CLT assumptions have been obtained by application of a penalty technique to the shear correction factor: the value $\chi = 1000$ will be used in the subsequent investigations. Lines and dashed lines are used to indicate FSDT and CLT solutions, respectively. All of the results in the figures take the form of load parameter λ vs transverse displacement at the plate center W_c. For our purpose and also because large rotations are not considered herein, values of W_c lower than $3h$ are investigated. We make note that W_c is not always coincident with the maximum normal deflection of the plates (in fact, the location of the maximum transverse deflection depends on both mechanical properties and boundary conditions). The FSDT results are referred to the value $\chi = 5/6$ of the shear correction factor. To compare results related to the same level of FEM accuracy, always full plates are analyzed even in those cases in which a quarter of plate should be enough. In the end we remark that all of the investigations have been performed on a PC 486 and to trace each curve has requested some CPU minutes. Assessment of the model herein used has been presented in the already cited authors' works. We refer to a regular mesh with 14×14 $Q4$ elements.

Figure 1 compares the postbuckling responses of the described laminated plates. Results are plotted and the four different boundary
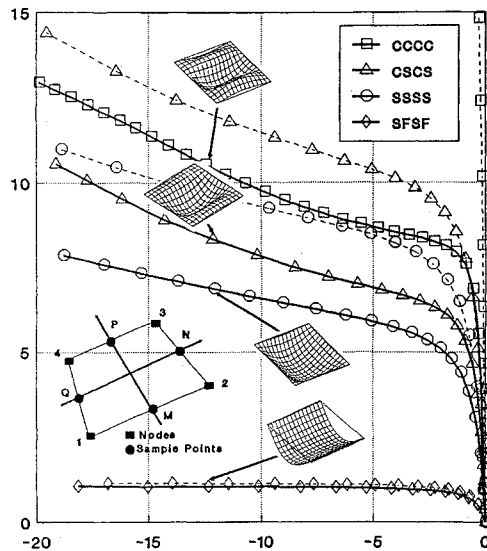
Fig. 1 Influence of boundary conditions for orthotropic plates; LAM1, FSDT and CLT solutions.

Fig. 2 Influence of the ratio E^S/E_l^P on the behavior of an SSSS plate with LAM1 layup; FSDT and CLT solutions.

conditions are considered. For buckling and postbuckling responses we confirm the well-known results from both buckling[1] and postbuckling[6] analyses: W_c increasing the equilibrium states depends on both lamination schemes and boundary conditions; transverse shear deformations are very much subordinate to boundary conditions. We underline that compressive loads have been applied by a constant distribution at the two loaded edges. These loads uniformly increase by λ parameter as stated in Sec. II. Some buckled modes for the several equilibrium points are also depicted inside Fig. 1. It is to be pointed out that, for the case of SFSF boundary conditions, i.e., beam case is simulated, the von Kármán nonlinear model, in conjunction with the used $Q4$ linear element, shows some limitations in the large deflection field (see also Fig. 4). This fact is well known in the literature; see Ref. 8. We notice that being $Q4$ an element that has linear interpolation then the clamped boundary conditions are not evident in the plotted shapes. Besides, as found in Ref. 16 (where exact solutions for buckling and vibration of panels are considered) and Ref. 14 (where postbuckling is studied), the deformation modes could be different between FSDT and CLT analyses. The term W_c increasing the plates tends toward a not constant distribution of the in-plane displacements at the edges. Because of edges effects and in correspondence to the edges center ($x = a/2; y = 0, b$) the used model leads to greater values of in-plane displacements v in respect to those in the neighborhood of $x = 0, a$. Such a behavior already observed in Refs. 10 and 15 is not completely realistic. In practice, aerospace constructions, e.g., wing or fuselage panels, are usually bounded by stiffeners along their edges. The stiffness of the stiffeners cannot be neglected, especially for panels bounded by longerons. Further stiffeners usually bound panels along their two sides. That is, in the postbuckling range stiffeners constrain the plates edges to maintain a constant displacements distribution rather than a uniform loads distribution. A more realistic modeling of the edges constraint is discussed in the subsequent analyses.

First, one remarks that in the linear analyses or in the buckling of plates (classical bifurcation analysis of Euler type), the distribution of the load along the plate edges that leads to a constant distribution of the correspondent in-plane displacements is necessarily assumed load level independent. In fact, in a classical eigenvalues analysis this distribution increases by means of a load factor until a bifurcation point has been reached. In the analyses in Fig. 1 we have done the same; in fact, in our FEM formulation the loads increase by means of the load parameter λ. But in the large deflections range, the loads distribution necessary to maintain a uniform distribution of the edge displacements should be load level dependent. To consider effects related to the stiffeners, one adds to the FEM mesh (as done in Ref. 15), and in correspondence to the loaded
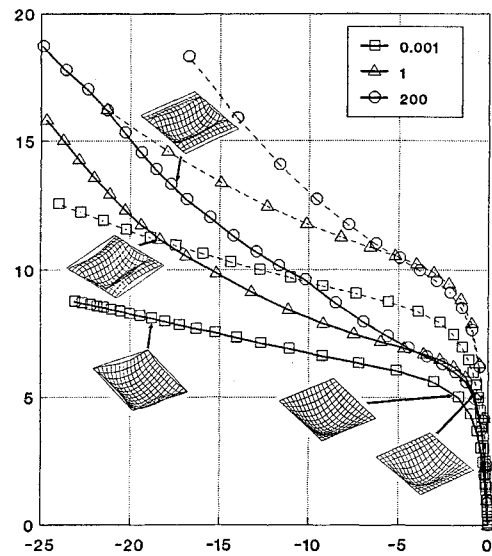
edges, two rows of $Q4$ plate elements (which could have different Young modulus E^S values in respect to the reference E_l^P value of the plate); see the sketches in Fig. 2. The stiffeners have been simulated by isotropic plates. By varying E^S/E_l^P the model should be able to enforce a constant distribution of the displacements along the loaded edges. We make note that with E^S increasing then the applied loading N_{yy} could be simulated by application of the resultant value N_{yy} directly at the plate edge centers. Three different boundary conditions have been investigated and three very different behaviors have been discovered. Figure 2 considers the case of simply supported. The different curves show that both prebuckling and buckling responses are affected by E^S/E_l^P ratio. But deflections increasing the differences among the several curves tragically grow up.

In addition we observe that E^S/E_l^P increasing the postbuckling of simply supported plate tends toward CSCS plate for both CLT and FSDT cases (see Fig. 1). In fact, with stiffeners' stiffness increasing, then the rotations at the loaded edges are enforced to be zero in our finite element model; i.e., the simply supported constraint tends to coincide to the clamped one. This fact becomes more evident by looking at the shapes quoted inside Fig. 2, where some FSDT buckled and postbuckled equilibrium states are drawn. Besides E^S/E_l^P increasing, the constant distribution of v displacements at the loaded edges becomes evident. We can conclude that in the case of simply supported edges the difference of the postbuckling behavior in respect to the analysis done at Fig. 1 should be charged of the following reasons: 1) the stiffeners constrain the edges to have a constant distribution of the displacements v; and 2) the stiffeners constrain the edge rotations to be very small so that the simply supported constraint cannot be simulated in both prebuckling and postbuckling range. Because of 1, Fig. 2 doesn't lead exactly to the CSCS results at Fig. 1. On the other hand, the case $E^S/E_l^P = 0.001$ in Fig. 2 exactly coincides with the SSSS case in Fig. 1. Same analyses have been conducted at Fig. 3, where clamped plates are considered. The same conclusions of the previous analysis can be extended to these cases with the following differences: given that the plates are already clamped, the stiffeners only provide constant distributions of displacements along the loaded edges. In this case the prebuckling and buckling solutions are not affected by E^S/E_l^P ratio. In fact, as recalled at the beginning of this subsection, given that the buckling loads correspond to a bifurcation from the undeformed state, then it cannot lead to different results when constant distributions of displacements or loads are considered at the loaded edges. Figure 3 shows that the postbuckling range could be tremendously different. Results related to the third investigated case are considered in Fig. 4, which compares stiffeners effects for plates simply supported at the loaded edges and free at the two others. Given that the loaded
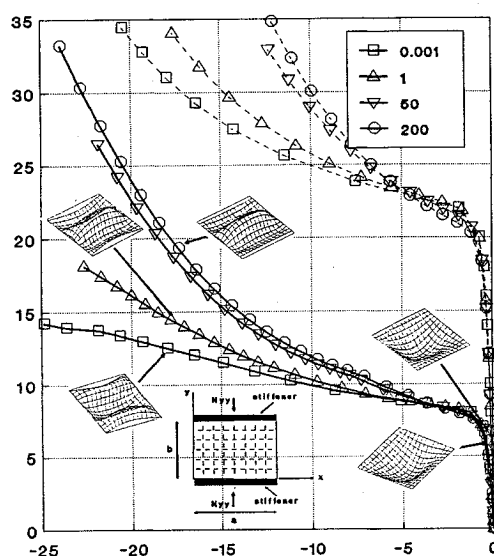
Fig. 3　Influence of the ratio E^S/E_l^P on the behavior of a CCCC plate with LAM1 layup; FSDT and CLT solutions.
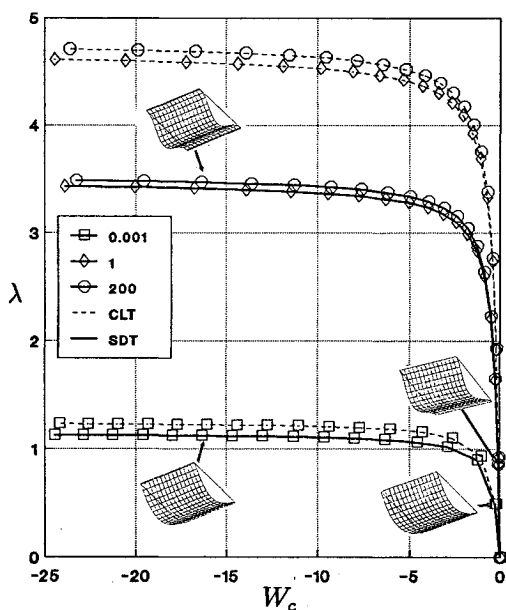

Fig. 4　Influence of the ratio E^S/E_l^P on the behavior of an SFSF plate with LAM1 layup; FSDT and CLT solutions.

edges are simply supported, then the conclusions reached at Fig. 2 can be redrawn. In fact, the shapes plotted inside Fig. 4 show that with E^S/E_l^P increasing the simply supported edges tend toward the clamped one. Different behavior in respect to the two previous analyses has been found in the postbuckling range. Because of the free edges, in this third case reason 2 becomes weaker in respect to the other two cases, and the relative differences among the several curves at Fig. 4 become nearly constant in the postbuckling range. We can conclude that postbuckling range is very much affected by stiffeners' stiffness; besides it tremendously depends on the considered boundary conditions. In fact, very different behavior has been found by comparing results from Figs. 1 to 4. We notice that it is not obvious to establish which one of the two extreme investigated simulations is the most realistic: the geometrical one, i.e., constant distribution of displacements along the edge, or the mechanical one, i.e., constant distribution of the compressive loads. Very probably the effective one is in between. But we can certainly conclude that in the nonlinear field much more care must be given to the manner in which boundary conditions are simulated. Besides stiffeners could improve very much the postbuckling strength of composite

flat panels. In the end we point out that our model used to simulate stiffeners also enforces constraint of other components of the displacements (u and ϕ_y) at the plates' loaded edges. Furthermore, stiffeners should also be introduced also in correspondence to the not loaded edges.

From the analyses conducted we make the following remarks.

1) The finite element method is a very versatile tool to simulate the response of different boundary conditions of flat panels. Furthermore, it easily permits the simulation of stiffeners effects.

2) The importance of both postbuckling analyses and shear deformation effects have been confirmed in thick plates studies.

3) In respect to prebuckling and buckling analyses, much more care should be taken to simulate constraints at the loaded plate edges. In fact, very different postbuckling results can be obtained when constant distributions of in-plane displacements and in-plane compressive loadings are imposed at these edges. Moreover, to accurately predict the stress-strain fields in the nonlinear range, HSDT effects should be included in the formulations. But to this purpose, first the possibility of developing a computationally robust finite element, including HSDT effects, should be investigated. Further, very useful conclusions could be reached by considering different loading conditions. These could be subjects for future work.

References

[1]Leissa, A. W., "Buckling of Laminated Plates and Shell Panels," Flight Dynamics Lab. Rept. AFWAL-TR-85-3069, 1985.

[2]Chia, C. Y., Nonlinear Analysis of Anisotropic Plates, McGraw-Hill, New York, 1980.

[3]Starnes, J. M., Jr., Knight, N. F., Jr., and Rouse, M., "Postbuckling Behavior of Selected Flat Stiffened Graphite-Epoxy Panels Loaded in Compression," AIAA Journal, Vol. 23, No. 8, 1985, pp. 1236–1246.

[4]Chai, C. B., Banks, W. M., and Rhodes, J., "An Experimental Study on Laminated Panels in Compression," Composite Structures, Vol. 19, No. 1, 1991, pp. 67–87.

[5]Chia, C. Y., "Geometrically Nonlinear Behavior of Composite Plates: A Review," Applied Mechanics Review, Vol. 41, 1988, pp. 439–450.

[6]Librescu, L., and Stein, M., "Postbuckling Behavior of Shear Deformable Composite Flat Panels Taking into Account Geometrical Imperfections," AIAA Journal, Vol. 30, No. 5, 1992, pp. 1352–1360.

[7]Librescu, L., and Chang, M. Y., "Imperfections Sensitivity and Postbuckling Behavior of Shear Deformable Composite Doubly Curved Shallow Panels," International Journal of Solids and Structures, Vol. 29, No. 9, 1992, pp. 1065–1083.

[8]Crisfield, M. A., Non-Linear Finite Element Analysis of Solids and Structures, Wiley, London, 1992.

[9]Dvorkin, E. N., and Bathe, K. J., "A Continuum Mechanics Based Four-Node Shell Element for General Non-Linear Analysis," Engineering Computations, Vol. 1, No. 1, 1984, pp. 77–88.

[10]Carrera, E., "Postbuckling Behavior of Multilayered Shells (in Italian)," Ph.D. Thesis, DIAS, Politecnico di Torino, Torino, Italy, 1991.

[11]Carrera, E., "On the Non Linear Response of Asymmetrically Laminated Plates in Cylindrical Bending," AIAA Journal, Vol. 31, No. 7, 1993, pp. 1353–1357.

[12]Carrera, E., "A Study on Arc-Length-Type Methods and Their Operation Failures Illustrated by a Simple Model," Computer and Structures, Vol. 50, 1994, pp. 217–229.

[13]Carrera, E., "On a Simple Finite Plate Element Computationally Efficient and Able to Include HSDT Effects," Aerotecnica Missili e Spazio, Vol. 73, Nos. 1–2, 1994, pp. 14–21.

[14]Carrera, E., and Villani M., "Large Deflections and Stability FEM Analysis of Shear Deformable Compressed Anisotropic Flat Panels," Composite Structures, Vol. 29, 1994, pp. 433–444.

[15]Carrera, E., "Non-Linear Analysis of Shear Deformable Plates," International Council of the Aeronautical Sciences, Vol. 3, ICAS-94-9.8.2, 1994, pp. 2964–2974.

[16]Carrera, E., "The Effects of Shear Deformation and Curvature on Buckling and Vibrations of Cross-Ply Laminated Composite Shells," Journal of Sound and Vibration, Vol. 150, No. 3, 1991, pp. 405–433.